



# THE USE OF AN EQUIVALENT FORCES METHOD FOR THE EXPERIMENTAL QUANTIFICATION OF STRUCTURAL SOUND TRANSMISSION IN SHIPS

M. H. A. JANSSENS, J. W. VERHEIJ

*TNO Institute of Applied Physics, P.O. Box 155, 2600 AD Delft, The Netherlands*

AND

D. J. THOMPSON

*Institute of Sound and Vibration Research, University of Southampton, Highfield,  
Southampton SO17 1BJ, England*

*(Received 9 December 1998, and in final form 29 March 1999)*

Structure-borne sound transmission is a complex phenomenon, the accurate measurement of which requires advanced techniques. A multi-dimensional substitution source method is presented by which structure-borne sound transmission paths can be quantified in practical situations where it is not possible to dismount the paths. The paper illustrates, by means of two examples, that reasonable results can be obtained using a suitable choice of force and response positions that are accessible in a practical situation. Additionally, techniques for quantifying confidence intervals are developed. Results are presented for the application of the method to sound transmission along realistic laboratory models of a ship drive shaft and a fluid-filled piping system. It is shown that the use of such a multi-degree-of-freedom approach to mechanical substitution sources is essential in the applications considered. For the drive shaft, the transmission through a bearing can be reproduced satisfactorily by two excitation degrees of freedom, but for the pipe even six was insufficient. Finally, numerical simulations are used to demonstrate that this is a result of transmission through the water within the pipe and that use of more excitation degrees of freedom would allow it to be taken into account.

© 1999 Academic Press

## 1. INTRODUCTION

The installation of machinery, such as propulsion or auxiliary diesel engines, within ship structures inevitably leads to the transmission of sound to accommodation areas within the ship as well as into the water. For both civilian and military vessels it is important to minimize this noise and in order to do so effectively it is essential that the contributions of the dominant sources and transmission paths can be

distinguished and quantified. Sound from machinery in ships is transmitted via a number of paths [1]. In the course of time, the contribution from the mechanical path through the engine mounts has been reduced by more effective resilient mounting strategies. Consequently, flanking paths have become more important. These include exhaust systems, vibration transmitted through drive shafts, cooling water pipes, etc. and airborne sound radiated from the engine structure into the engine room.

Traditional experimental techniques for quantifying sound transmission paths involve isolating paths by means of progressively uncoupling connections or shielding air-borne radiation and then monitoring the differences in sound transmitted. Their accuracy is limited by restrictions in the isolation which is possible. In an environment where multiple paths contribute significantly, the resolution can be compromised by the contribution from a single path for which the achievable isolation is limited.

Substitution source techniques are commonly used in quantifying air-borne sound transmission paths in many applications. The underlying principle is to generate in situ the same source strength as the actual source by using artificial excitation, e.g. loudspeakers. The sound pressure measured at the point of interest can then be equated to the air-borne contribution alone and other components are completely eliminated. There are, of course, attendant problems of defining and measuring the source strength of the actual source, but practical solutions to these problems are well documented [2].

Similar techniques have also been exploited for evaluating the contributions of structure-borne paths. In this case, the source of structure-borne sound transmission, e.g. the engine, is replaced by a mechanical substitution source, such as an exciter, at the same mounting point. If this is then driven at the "source" level of the original source, the contribution at the receiver position can be equated with the structure-borne path. Similar problems exist as with acoustical substitution sources, although their solution is more elusive. For example, the definition of a universal source strength which is appropriate for mechanical sources is still a matter of considerable research [3]; it is generally necessary to consider multiple directions of excitation, and the relative amplitudes and phases of the source and receiver structure impedances.

The method which is studied in this paper is effectively an advanced mechanical substitution source method. Its purpose is to account experimentally for the multi-dimensional nature of many instances of structure-borne sound transmission and yet to overcome the requirement physically to remove the source for parts of the measurement programme. The method has a number of features in common with inverse methods of force identification and also with active control of noise and vibration. These will be discussed in section 2.2, after the method has been presented.

Similar methods, commonly referred to as "transfer path analysis" have become widely used in recent years, particularly for road vehicle applications [4-8]. These are usually based on a determination of the actual forces acting at structural mounting points of a noise source. The forces can be determined either by measuring the relative motion across a resilient mount and using this in

conjunction with a known stiffness, or more generally a matrix of transfer impedances, or by inversion of a matrix of frequency response functions measured on the receiver structure. The forces are then used in combination with a set of transfer functions to derive the sound pressure at the receiver location.

The method described here is essentially similar to this latter method, with the exception that the forces applied here are not limited to the mounting points of the source structure. By removing this requirement, the source can usually be left in situ, though not operational, during the transfer function measurements.

The purpose of this paper is to describe the use of such a multi-dimensional mechanical substitution source method, applicable under practical field conditions where it is not possible to dismount the structural paths. The number and location of force and response positions required is illustrated by means of two practical examples. Moreover, a methodology for determining confidence intervals of the results is developed which to the authors' knowledge has not previously been published in this context.

The paper describes applications carried out in a laboratory environment on structures that are typical of those found on board ships. Subsequently, the method has been applied to various paths on a ship and has been shown to be viable [9]. Although the work described has been aimed at applications to ships, the method has wide potential in other areas where structural sound transmission has to be quantified experimentally, such as in road vehicles, trains, aircraft and buildings.

## 2. THE EQUIVALENT FORCES METHOD

### 2.1. PRINCIPLE OF THE METHOD

Consider a notional source of structurally transmitted sound shown in Figure 1. This transmits sound to the receiver position, shown here underwater, by a variety of paths. For example, for an engine on a ship, these paths include the resilient mounts, the cooling water pipes and the drive shaft. The definition of a "path" here depends on the purpose of the experiment. For example, the various resilient mounts could be considered as a single "path" or as separate "paths" depending on whether the whole sound transmission through the mounts is to be determined or whether the relative contribution of each mount is required. Similarly, a pipe could be considered as a single path in which all of its degrees of freedom are included, or as a combination of paths related to different wave types or as part of a path that includes other pipes or other types of connection between the source and receiver structure.

The method consists of a set of measurements performed with the machine running (see Figure 1(a)), a second set of measurements with the machine stationary (see Figure 1(b)) and an analytical step combining the results, which need not be carried out at the time of the measurements.

Whilst the machine is running, a series of operational responses, such as accelerations, are measured at positions which characterize the path in question. They do not have to be adjacent to the connection points between source and receiver. The machine response is assumed to be stationary and the responses are

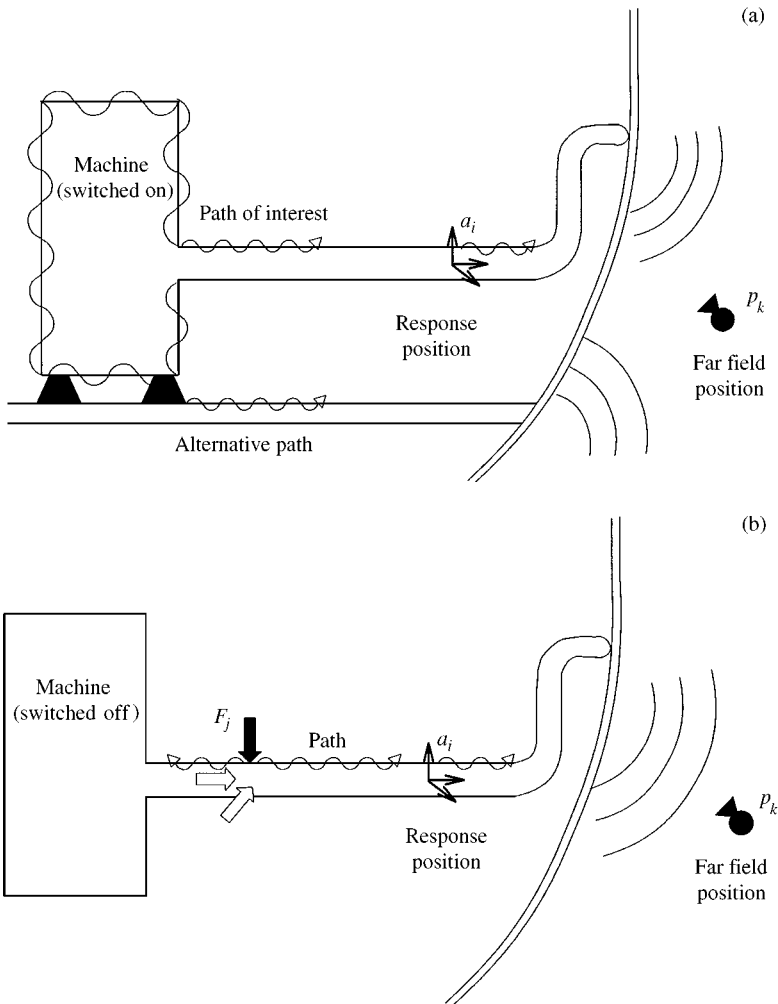


Figure 1. Schematic representation of the method. (a) Machinery vibration is transmitted along various paths to the far field positions. Responses  $a_i$  are monitored. (b) The sound transmitted along the path of interest is reconstructed using a series of equivalent forces  $F_j$ , derived from acceleration measurements  $a_i/F_j$ .

denoted by  $\{a_i(f)\}_{mach}$  where  $f$  is the frequency. These quantities have their phase referenced to one measurement point, without loss of generality, taken to be  $i = 1$ . They can be derived from the auto- and cross-spectra as

$$a_i(f) = \sqrt{G_{ii}} e^{j\angle(G_{i1})}, \quad (1)$$

where  $G_{ii}$  is the auto-power spectrum of the response at position  $i$  and  $\angle G_{i1}$  is the phase angle of the cross-spectrum between the reference positions 1 and  $i$ . The responses  $\{a_i\}_{mach}$ , are all assumed to be coherent. It is possible, in an extension of the method, to consider multiple uncorrelated sources, using a principal component analysis [2, 5, 10, 11].

The sound pressure, or other response quantity, at the receiver locations is also measured, denoted by  $\{p_k(f)\}_{total}$ , the index *total* indicating that the total response is measured due to the contributions of all paths, structure-borne and air-borne.

Then the machine is switched off and a series of force positions are selected which lie between the source and the operational response positions. The selection of force and response positions will be discussed later, but it may be noted that the force positions also do not have to lie at the interface of the source and the receiving structure. There should be enough force positions to allow the vibration field in the path in question to be reproduced, but they should not excite any other path significantly, i.e. the excitation should be only of the component or components of sound transmitted along the path under study. Transfer functions  $A_{ij} = a_i/F_j$  are then measured between each force position,  $j$  and each operational response position,  $i$ , and also between the force positions and the receiver locations,  $H_{kj} = p_k/F_j$ . For practical reasons it is often convenient to measure these transfer functions reciprocally. Recent overviews of application aspects of the use of reciprocity in such measurements are found in references [9, 12, 13]. In the case of accelerances, the force and response positions can simply be reversed,  $A_{ij} = a_i/F_j = a_j/F_i$ . In the case of transfer functions from force to sound pressure, the appropriate reciprocal relation is between the volume acceleration  $Q_k$  at the position  $k$  and the acceleration  $a_j$  at position  $j$ ,  $H_{kj} = p_k/F_j = a_j/Q_k$ .

The analytical step consists of determining the amplitude and phase of a set of equivalent forces,  $\{F_j\}_{eq}$ , which when applied at the positions  $j$  would reconstruct the vibration field due to the machine,  $\{a_i\}_{mach}$  as closely as possible. This is given by

$$\{F_j\}_{eq} = [A_{ij}]^{-1} \{a_i\}_{mach}, \quad (2)$$

provided that the matrix inversion can be performed. The issue of the validity of the matrix inversion is considered in detail below. The response at the receiver locations,  $k$ , due to the path in question can then be derived from

$$\{p_k\}_{path} = [H_{kj}] \{F_j\}_{eq}. \quad (3)$$

This can be combined with equation (2) to give

$$\{p_k\}_{path} = [H_{kj}] [A_{ij}]^{-1} \{a_i\}_{mach}, \quad (4)$$

from which it can be seen that the equivalent forces,  $\{F_j\}_{eq}$ , are required only as an intermediate parameter and are not of interest in themselves. The final result,  $\{p_k\}_{path}$  can be compared with the measured total response  $\{p_k\}_{total}$  to evaluate the importance of the path in question at the receiver location  $k$ . The contributions from several paths can also be added or compared.

## 2.2. DISCUSSION

The above procedure has similarities to the problem of active noise and vibration control. In that case, however, the forces  $\{F_j\}_{eq}$  would be introduced

simultaneously with the machine source and with an opposite phase in order to minimize  $\{p_k\}$ . The other main difference in the current situation is that the forces need not be calculated in real time, releasing the requirement to find an appropriate control algorithm.

As noted in the introduction, the method is also very similar to inverse methods for force determination based on response measurements and the inversion of a matrix of frequency response functions [5, 6, 14]. A wide range of applications of this procedure, popularly known as transfer path analysis, involve the use of these indirectly determined forces along with a matrix of vibro-acoustic transfer functions to quantify structure-borne sound transmission [4–8]. The method described here is similar to this latter method, but with the important generalization that the equivalent forces need not be placed at the interface points and therefore have no particular physical significance.

### 2.3. MATRIX INVERSION

An important aspect in the above is the need to invert a matrix containing measured data. This is essentially ill-conditioned even if the degrees of freedom are chosen to be theoretically independent [14, 15]. In order to improve the conditioning, the system may be overdetermined, that is the number of response positions,  $n$ , is chosen to be greater than the number of force positions,  $m$ . This can help to reduce problems caused by the presence in the matrices at some frequencies of very small terms corresponding to local anti-resonances. Nevertheless, Roggenkamp and Bernhard [16] have pointed out that overdetermination is only worthwhile if it improves the condition number of the matrix to be inverted. For the case  $n \neq m$ , the matrix inverse in equation (3) and (4) needs to be redefined as a least-squares pseudo-inverse.

A convenient method for obtaining a pseudo-inverse whilst avoiding problems with near-singularities is the singular value decomposition [17]. The matrix  $[A]$  is written in the form  $[A] = [U][S][V]^H$  in which  $U$  and  $V$  are transformation matrices satisfying  $[U]^H[U] = I$  and  $[V]^H[V] = I$  with  $I$  the unit matrix and  $S$  is diagonal with all diagonal terms  $s_i \geq 0$ . For convenience these terms, known as singular values, are arranged in descending order. The pseudo-inverse is formed as  $[A]^+ = [V][S]^+[U]^H$  with  $[S]^+ = \text{diag}(s_1^{-1}, \dots, s_r^{-1}, 0, \dots, 0)$  where  $r$  is the rank of  $A$ . Singular values which are small and therefore dominated by measurement error can be set to zero in the inverse preventing their dominance of the solution.

In order to use this effectively, a method of rejecting small singular values is required. For this, a method proposed by Powell [18, 19] has been used. This allows the threshold to be set according to the likely errors in the matrix  $[A_{ij}]$ . The coherence function  $\gamma_{ij}^2$  can be used as an indicator of the presence of random errors in  $A_{ij}$ , due to noise. Provided that the accelerances are measured when using random excitation, the coherence function can also be used to indicate bias errors in  $A_{ij}$ , such as due to leakage in the presence of lightly damped modes (i.e. where the impulse response function does not decay sufficiently within the analysis window).

For impact excitation, however, it should be noted that the coherence can be unity even in the presence of such bias errors. An error matrix  $E_{ij}$  is formed,

$$E_{ij} = 3 \{(1 - \gamma_{ij}^2)/(2n_{av}\gamma_{ij}^2)\}^{1/2} |A_{ij}|, \quad (5)$$

which is three times the standard deviation in  $A_{ij}$ , where  $n_{av}$  is the number of averages taken in estimating  $A_{ij}$  and the factor 3 is chosen as in references [18, 19] as a conservative estimate of the error, meaning that, for a normal distribution, there is a 99.7% probability that the measured function  $A_{ij}$  is within  $E_{ij}$  of the true value. The overall estimate of the error threshold is given by the norm of  $E_{ij}$ ,  $\varepsilon = \|E_{ij}\|$ . This is used in rejecting singular values of  $[A_{ij}]$ , i.e. if  $s_i < \varepsilon$ ,  $1/s_i$  is set to zero in the inverse. Such a method is considered more justified than using an arbitrary trigger level, such as 10% of the maximum singular value as used e.g. by Romano and López [7]. Finally, it should be remarked that it would be pointless to set all of the singular values to zero if they were all less than the error threshold, since this would lead to zero equivalent forces. A better solution, according to Powell [18] is to replace the largest singular value by the error threshold  $\varepsilon$  itself.

#### 2.4. CONFIDENCE INTERVALS

The prediction of the equivalent forces  $\{F_j\}_{eq}$  and the response at the receiver positions,  $\{p_k\}_{path}$ , is subject to several sources of error. Random errors in  $[A_{ij}]$  are accounted for by the threshold for rejecting singular values discussed above. The transfer functions  $[H_{jk}]$  will also contain random errors but these are not considered here. The following discussion is limited to the effect of random errors in the measured responses  $\{a_i\}_{mach}$  and of the uncertainty introduced by the pseudo-inversion. Errors may also be introduced by the selection of force and response positions but it is only partly possible to quantify these.

To derive confidence intervals relating to uncertainties in the responses measured while the machine is running,  $\{a_i\}_{mach}$ , a covariance matrix is determined,  $[C_{aa}]_{mach}$ . To determine a covariance of complex quantities, it is necessary to partition each term of  $\{a_i\}_{mach}$  into real and imaginary parts. This is because the covariance between two complex variables needs to account for four components,  $C_{Re,Re}$ ,  $C_{Re,Im}$ ,  $C_{Im,Re}$  and  $C_{Im,Im}$  whereas a single "complex covariance" could only have two independent components (its real and imaginary parts). The partitioned covariance matrix,  $[C_{aa}]_{mach}$  is therefore  $2n \times 2n$  rewriting  $\{a_i\}_{mach}$  as a real vector of length  $2n$

$$\{b\} = [\text{Re}\{a_1\} \cdots \text{Re}\{a_n\} \text{Im}\{a_1\} \cdots \text{Im}\{a_n\}]^T, \quad (6)$$

and denoting the difference between the  $s$ th measured sample of  $\{a_i\}_{mach}$  and the average over all  $S$  samples,  $\bar{b}$ , by  $\Delta_s = \{b\}_s - \bar{b}$ , the covariance estimate can be expressed as

$$[C_{aa}] = 1/(S - 1) \Sigma \Delta_s \Delta_s^T. \quad (7)$$

In practice, rather than storing all data before analysis as implied by this, it is more efficient to process the data during acquisition and update the estimate of the covariance matrix after each sample has been taken. In this case  $\Delta_s$  is based on the running average not the mean over the whole population of samples.

When the partitioned covariance matrix  $[C_{aa}]$  is known it is possible to derive the corresponding partitioned covariances  $[C_{FF}]_{eq}$  of  $\{F\}_{eq}$  and  $[C_{pp}]_{path}$  of  $\{p\}_{path}$  by using (see reference [20])

$$[C_{FF}]_{eq} = \{[A_{ij}^p]^T [C_{aa}]^{-1} [A_{ij}^p]\}^+, \quad (8)$$

where  $+$  denotes pseudo-inversion and  $p$  denotes partitioning with respect to real and imaginary parts, and

$$[C_{pp}]_{path} = [H_{kj}^p][C_{FF}]_{eq}[H_{kj}^p]^T. \quad (9)$$

These represent the uncertainties in  $\{F\}_{eq}$  and  $\{p\}_{path}$  due to variations in the responses measured while the machine is running.

Another uncertainty in the prediction is caused by the pseudo-inversion in equation (3). The predicted responses  $\{a_i\}_{fit} = [A_{ij}]\{F_j\}_{eq}$  are not, in general, the same as the measured responses  $\{a_i\}_{mach}$  as they are based on a fit with fewer degrees of freedom than  $n$ . The imperfection in this fit can come, for instance, from the use of insufficient force positions to determine the vibration field fully. These effects can be simulated by using a ‘‘variance of the fit’’ [21]. The partitioned covariance matrix of  $\{a_i\}_{mach}$  is given by

$$[C_{aa}]_{fit} = \left[ \begin{array}{cc|cc} \ddots & & 0 & \ddots & 0 \\ & Var_{Re,Re,fit} & & & Cov_{Re,Im,fit} \\ 0 & & \ddots & 0 & \ddots \\ \ddots & & & 0 & \ddots & 0 \\ & Cov_{Im,Re,fit} & & & Var_{Im,Im,fit} \\ 0 & & \ddots & 0 & & \ddots \end{array} \right], \quad (10)$$

where

$$Var_{Re,Re,fit} = \Sigma \{Re(a_{i,mach} - a_{i,fit})\}^2 / (n - r), \quad (11a)$$

$$Var_{Im,Im,fit} = \Sigma \{Im(a_{i,mach} - a_{i,fit})\}^2 / (n - r), \quad (11b)$$

$$Cov_{Re,Im,fit} = \Sigma \{Re(a_{i,mach} - a_{i,fit})Im(a_{i,mach} - a_{i,fit})\} / (n - r), \quad (11c)$$

and  $r \leq m \leq n$  is the rank of  $[A_{ij}]$  as used in the pseudo-inversion. The covariance matrices in equations (7) and (10) can be combined to give a total covariance and this can be inserted in the estimates of error propagation in equations (8) and (9).



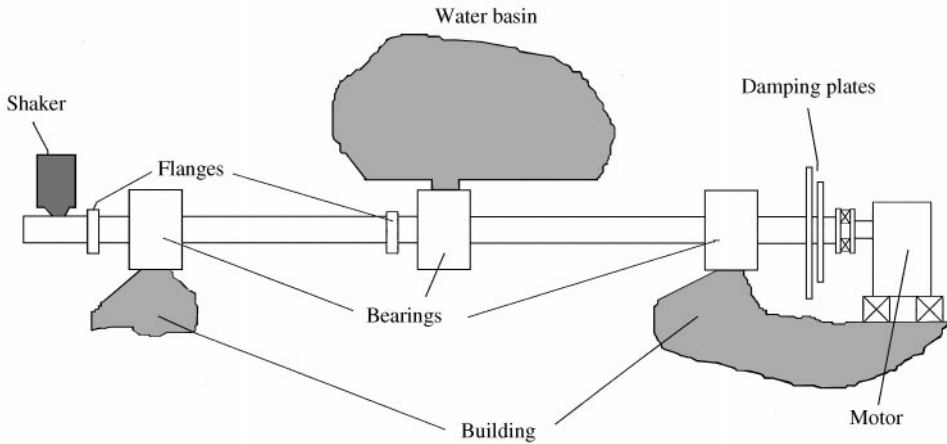


Figure 2. Overview of the scale model drive shaft.

Confidence intervals for the quantities  $\{F_{jj}\}$  and  $\{p_k\}$  can be derived from the respective covariance matrices by using a Monte Carlo technique.

### 3. LABORATORY EXPERIMENT ON DRIVE SHAFT BEARING

#### 3.1. TEST ARRANGEMENT

A scale model (scale  $\frac{1}{3}$ ) of a ship drive shaft has been constructed in the laboratory; see Figure 2. A shaker attached at one end of the shaft is used to simulate machinery-induced vibrations. This is inclined so that vibration is induced in the shaft in the vertical, lateral and longitudinal directions. At the other end a series of damped plates ensure dissipation and a net energy flow along the shaft. The shaft is supported on three journal bearings, and it is connected via the central one of these bearings to a reverberant water tank ( $360 \text{ m}^3$ ) the structure of which resembles a ship's hull. The other bearings are supported by the building, from which the water tank is dynamically uncoupled. By disconnecting the central bearing from the tank it was possible to show that structure-borne transmission through this bearing dominated the sound pressure under water in the tank in the frequency range up to 2 kHz. This allows the results from the method to be compared directly with the measured sound for validation purposes, as only the path under study is present.

A rather large set of force and response positions was chosen initially to enable various selection strategies to be investigated. Six force positions ( $F_1-F_6$ ) were chosen on the bearing housing, which represented combinations of the six rigid body motions of the bearing. Eleven accelerometer positions ( $a_1-a_{11}$ ) were chosen around the connection between the bearing support and the water tank. These are shown schematically in Figure 3. Four underwater receiver positions were used, distributed randomly through the tank.

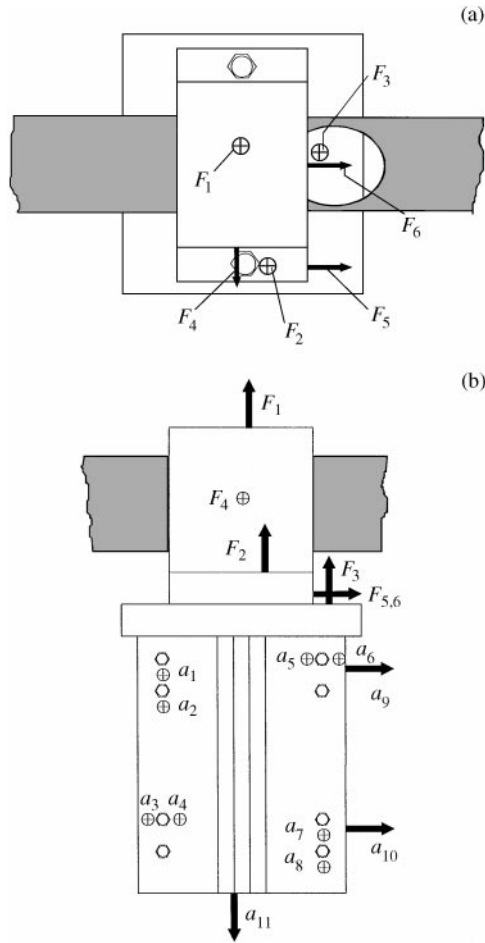


Figure 3. Force ( $F$ ) and acceleration ( $a$ ) positions at the central bearing. (a) Top view. (b) Side view.  $\oplus$  indicates force or response acting out of the plane.  $F_3$  and  $F_6$  are located below the shaft, shown cut away.

### 3.2. MEASUREMENTS

The accelerances  $[A_{ij}]$  were measured reciprocally by using hammer excitation. The force transducer was attached to the structure and was fitted with a rounded metal head. This was then excited by using a plastic headed hammer. In this way, the excitation was at a repeatable location, avoiding one of the major sources of inaccuracy in using hammer excitation. Figure 4 shows two examples of accelerances which indicate that the structure does not exhibit strong modal behaviour.

The sound transfer measurements  $[H_{kj}]$  from the six force positions to the four underwater locations were measured reciprocally by using a calibrated underwater sound source at each of the “receiver” locations in turn and measuring the transfer functions to the acceleration at each of the six “force” positions. As examples, two of

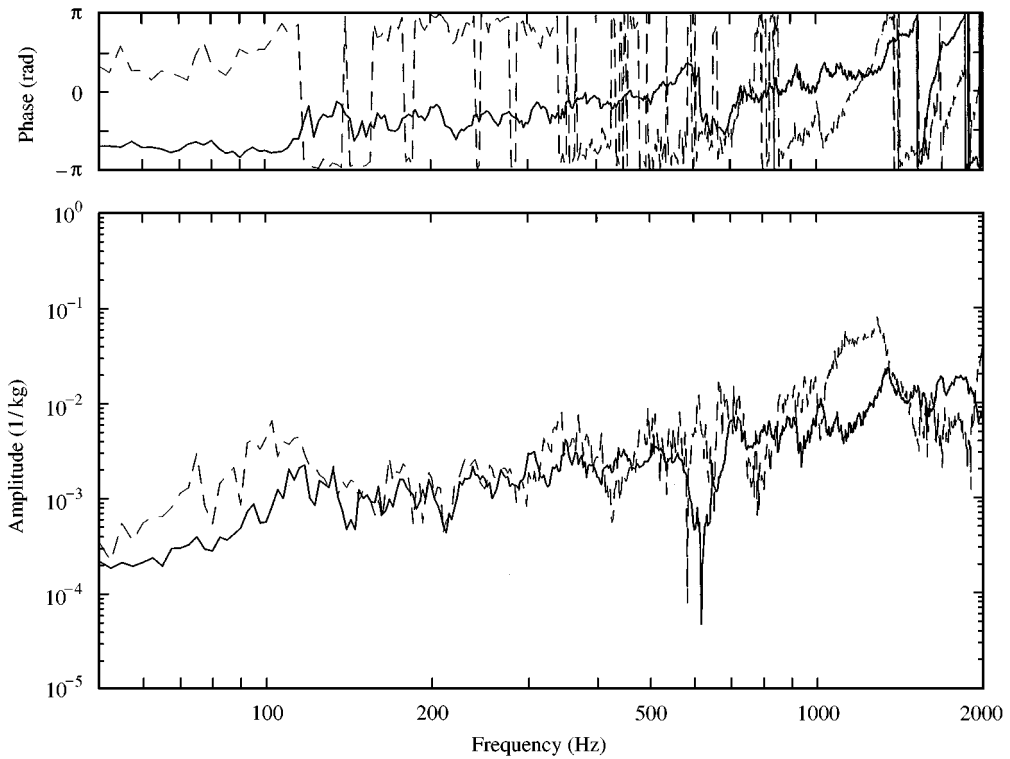


Figure 4. Example accelerances  $A_{ij}$  for the drive shaft: —,  $a_{11}/F_1$ ; ---,  $a_1/F_4$ .

these transfer functions are shown in Figure 5. The reverberant nature of the response of the tank can be clearly seen.

The 11 structural responses  $\{a\}_{mach}$  were measured with the shaker representing the “machine” source driven by a periodically swept sine signal with period 0.4 s. Its orientation ensured that the shaft was driven in the vertical, horizontal and longitudinal directions. The full covariance matrix  $[C_{aa}]_{mach}$  was measured in three parts as the data acquisition equipment was limited to eight simultaneous channels. All channels were carefully calibrated for amplitude and phase.

The underwater sound at the four receiver positions was measured by using hydrophones during operation of the “machine”,  $\{p_k\}_{total}$ . Since the path through the instrumented bearing dominates the transmission from the “machine” into the water, these measured pressures can be compared with those estimated from the method. All results are shown as the average of the four receiver positions.

### 3.3. RESULTS USING ALL FORCE AND RESPONSE POSITIONS

The results when using the full  $11 \times 6 [A_{ij}]$  matrix are shown in Figure 6 as  $\frac{1}{3}$  octave band spectra. Note, however, that all calculations are performed using

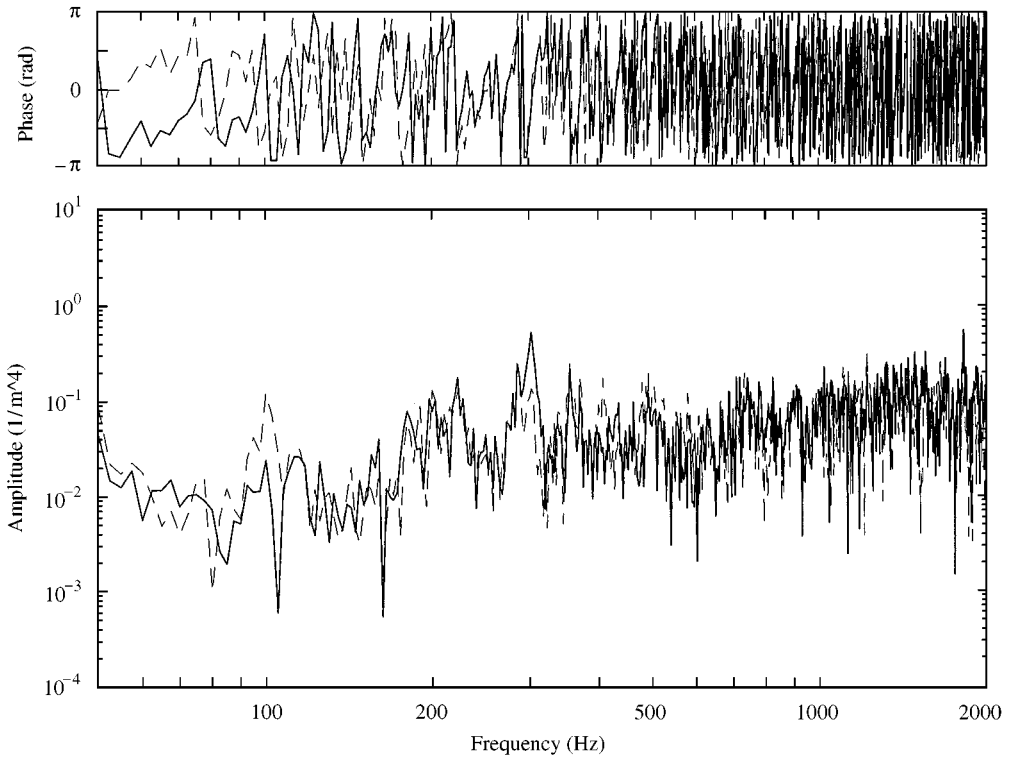


Figure 5. Example acoustical transfer function  $H_{kj}$  from the drive shaft to the water tank: -----,  $p_1/F_1$ ; ---,  $p_1/F_4$ .

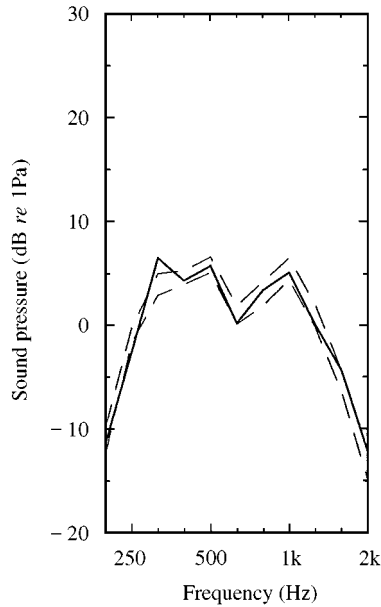


Figure 6. Results obtained for the drive shaft using the full  $11 \times 6 [A_{ij}]$  matrix: -----, measured; ---, calculated, 95% confidence interval.

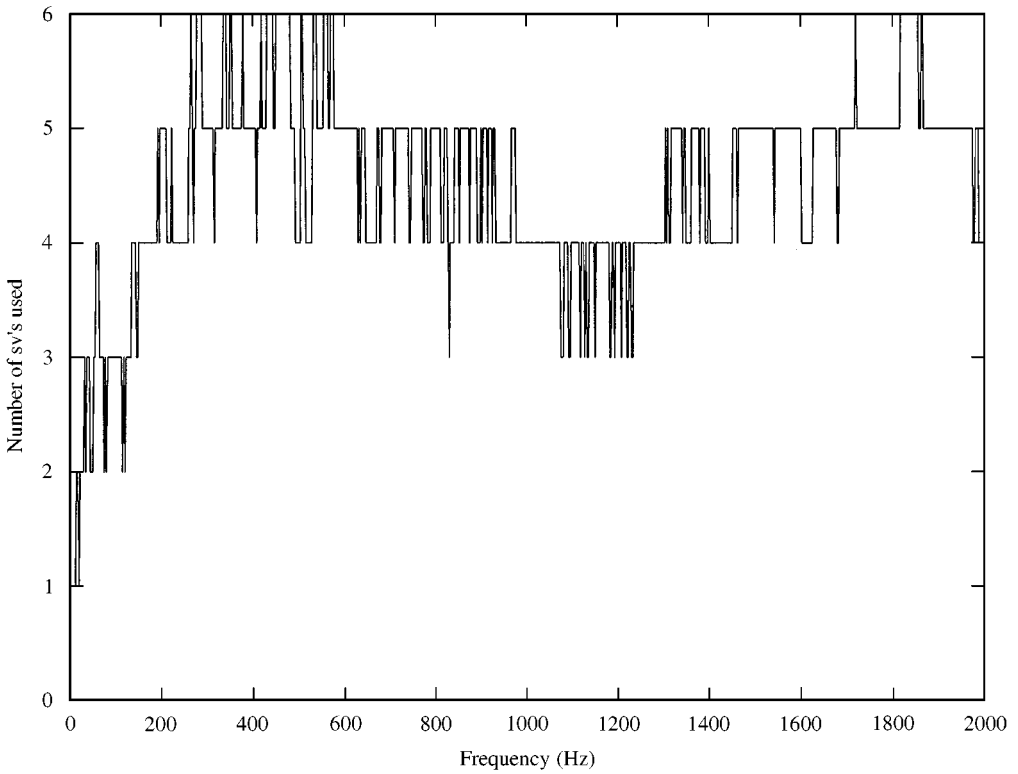


Figure 7. Number of singular values used for the drive shaft in the pseudo-inversion of the  $11 \times 6$   $[A_{ij}]$  matrix for each frequency.

narrow band data with a bandwidth of 2.5 Hz, the conversion to  $\frac{1}{3}$  octave bands being performed only on the final result. This allows the results to be seen more clearly, as the narrow-band results contain many peaks and troughs due to the reverberant nature of the tank (see Figure 5). The 95% confidence interval that has been derived from the covariance matrix is also shown. The calculated results agree very well with the measurements and although the confidence interval is small the measured result mostly falls within this confidence interval. Although both  $[C_{aa}]_{mach}$  and  $[C_{aa}]_{fit}$  were used (see section 2.4), it was found that, in this laboratory experiment, the confidence intervals were dominated by the latter, the artificial “machine” being very repeatable.

It was found that, according to the error threshold, mostly 4 or 5 singular values of  $[A_{ij}]$  were acceptable. The number of singular values used is shown in Figure 7. The matrix has the full rank of six at only a few frequencies at which the condition number of the original matrix is relatively low. By rejecting the unacceptable singular values the condition number is reduced at other frequencies by as much as a factor of 10 as shown in Figure 8. If the full matrix is used with no rejection of singular values, deviations in the  $\frac{1}{3}$  octave band sound pressures of up to 4 dB are found to occur.

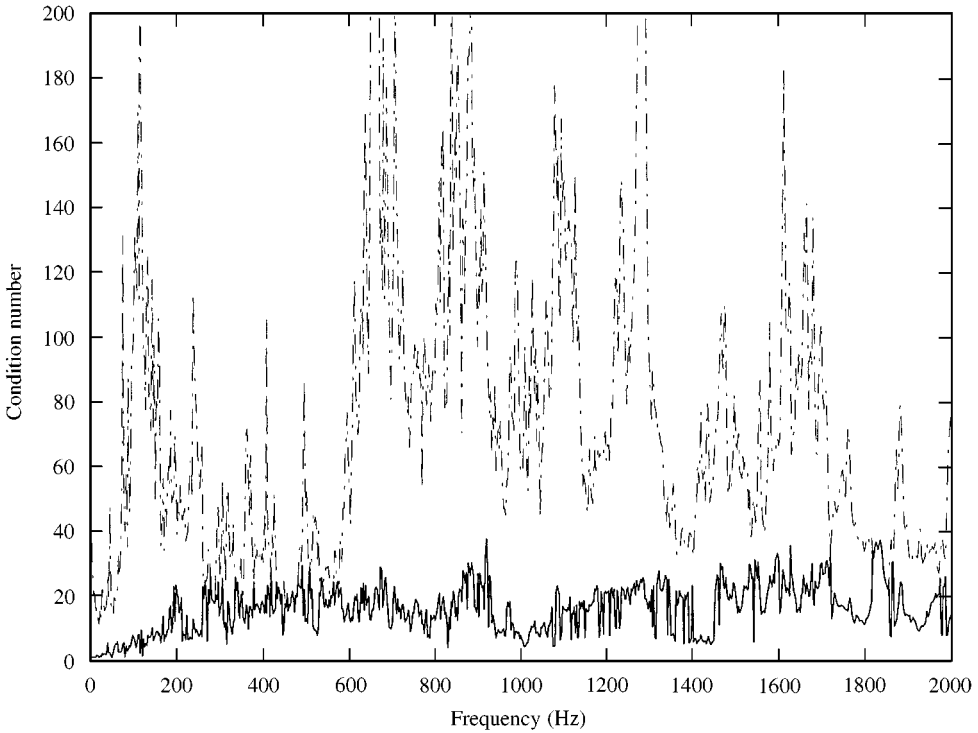


Figure 8. Condition number of the  $11 \times 6 [A_{ij}]$  matrix for the drive shaft: —, with all six singular values; ---, with singular values according to Figure 7.

### 3.4. RESULTS USING A SUB-SET OF POSITIONS

A number of cases of using sub-sets of response and/or force positions have been investigated. The results showed that rather good agreement could be obtained using a rather small set of force and response positions. Figure 9 shows the result obtained from a  $4 \times 2 [A_{ij}]$  matrix (forces 1 and 4 and responses 1, 2, 3 and 11, which were found to be the most important positions). Although the confidence intervals are wider than in Figure 4, the measured response is still contained within them. This suggests that the sound transmission through the bearing is dominated by vertical and lateral forces, whereas the important response of the mounting plate on the side of the tank is in the normal direction.

However, when reducing this further by using only a single force, it was found that significant errors occurred. Figure 10 shows the result for force 4 only, the most important single force. In this case the errors in the  $\frac{1}{3}$  octave spectra were as much as 9 dB. Similarly, Figure 11 shows the results of using two forces but neglecting their relative phase, the calculations being performed in  $\frac{1}{3}$  octave bands. Here too the errors were as much as 10 dB, in this case mostly an overprediction.

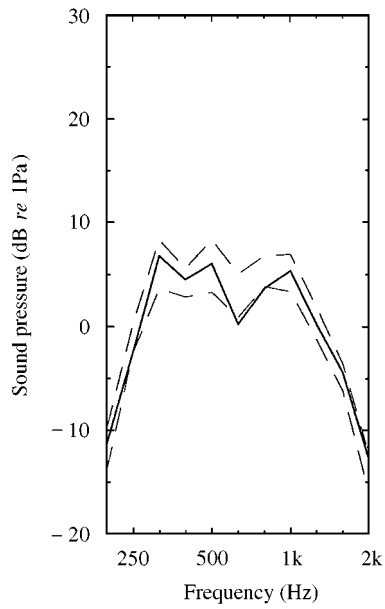


Figure 9. Results obtained for the drive shaft using  $4 \times 2 [A]_{ji}$  matrix: —, measured; ---, calculated, 95% confidence interval.

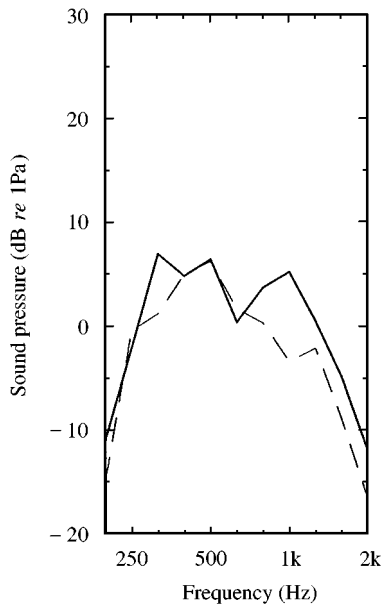


Figure 10. Results obtained for the drive shaft using only one force position ( $F_4$ ): —, measured; ---, calculated.

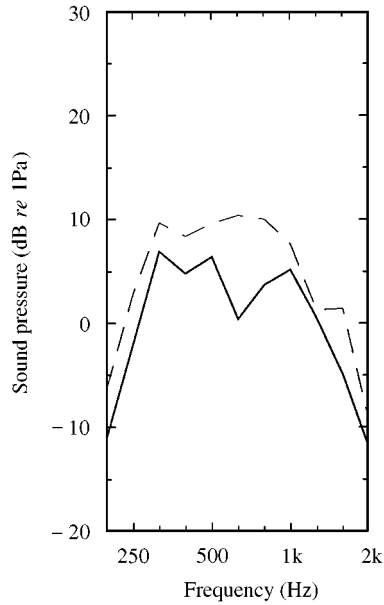


Figure 11. Results obtained for the drive shaft using only two force positions ( $F_1$ ,  $F_4$ ), calculations performed in  $\frac{1}{3}$  octave bands without phase information: ---, measured; —, calculated.

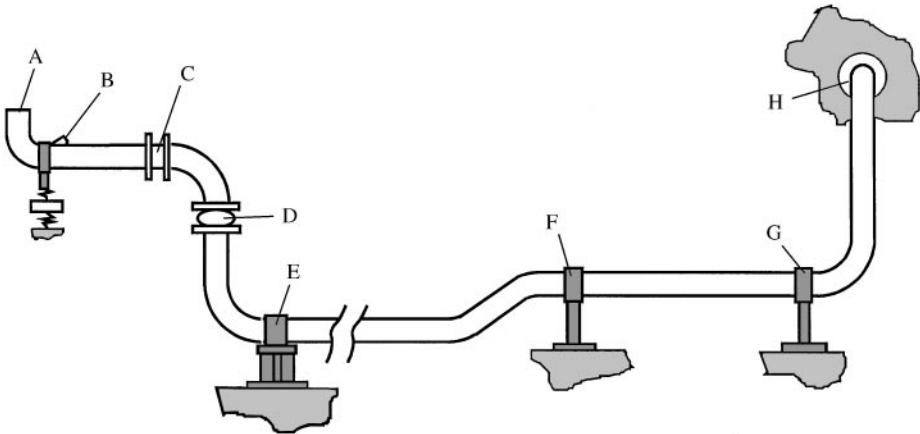


Figure 12. Diagram of the pipe system. A: termination. B: excitation using a shaker. C: joint with flanges. D: flexible bellows. E, F and G: brackets connecting pipe to the water tank. H: valve connecting pipe to the water tank.

#### 4. LABORATORY EXPERIMENT ON WATER-FILLED PIPE SYSTEM

##### 4.1. TEST ARRANGEMENT

A second set of laboratory measurements has been performed on an 8 m long non-planar fluid-filled pipe system, shown schematically in Figure 12. This represents the cooling water pipe of a ship diesel engine. It is connected to the hull



structure of the reverberant water tank via three brackets (E, F and G) and at its end (H) where a valve is located. With the valve open a connection to underwater is present via the fluid in the pipe. With the valve closed, the pressure of the water in the pipe can be increased by means of a hand-operated pump. The section of pipe on the source side of a bellows at D is not in contact with the tank except via resilient mounts. The system is excited by a mechanical shaker at B, mounted at an angle to the normal, which represents the “machine” source. It can be expected that the presence of bends, particularly in the source section, will lead to significant fluid-borne as well as structure-borne sound transmission. Because the pipe can be disconnected from the tank, it could be shown that sound transmission to underwater is sufficiently well dominated by the pipe path in the  $\frac{1}{3}$  octave bands 50–630 Hz inclusive. Therefore, again comparison with overall measurements allows validation of the method.

Six force locations were chosen on the flange directly downstream of the bellows at D. They were chosen to excite all six degrees of freedom of the flange when considered as a rigid body. A total of 14 response positions were chosen, five of which were at D. Three were orthogonal positions at E, two at F and one at G. Finally, three orthogonal positions at H were also included. No force or response positions were used in the fluid as these are more difficult to achieve, especially in a situation on board a ship.

#### 4.2. MEASUREMENTS

The  $14 \times 6$  accelerance matrix  $[A_{ij}]$  was measured with the water in the pipe not pressurized, which is the normal condition on a ship when the engine is not operating. Measurements were made using a plastic hammer to excite the structure through a force transducer attached to the flange. The accelerances were measured for frequencies up to 800 Hz at a resolution of 1 Hz. Example accelerances are given in Figure 13 from which it can be seen that the pipe response is somewhat more modal than that of the shaft (see Figure 4).

The  $2 \times 6$  matrix of sound transfer functions  $[H_{kj}]$  was measured reciprocally in the same way as for the drive shaft. For this a periodically swept sine excitation with period 1 Hz was used which was driven synchronously with the sampling.

In order to measure the responses during operation of the “machine” a 4 bar overpressure was applied to the pipe fluid, as would be the case in the situation on board a ship. The shaker representing the machine was driven with a periodically swept sine signal with period 0.16 s. The whole covariance matrix was not measured, but the partial covariance matrix was measured for two sub-sets of eight response positions. Set 1 comprised all positions at D and E, set 2 comprised the remainder plus two of the positions at D. The underwater sound was measured at the two hydrophone positions during operation of the “machine” source. As above, the calculations are performed by using narrow band data (bandwidth 1 Hz) but for presentation purposes the results are shown in  $\frac{1}{3}$  octave bands.

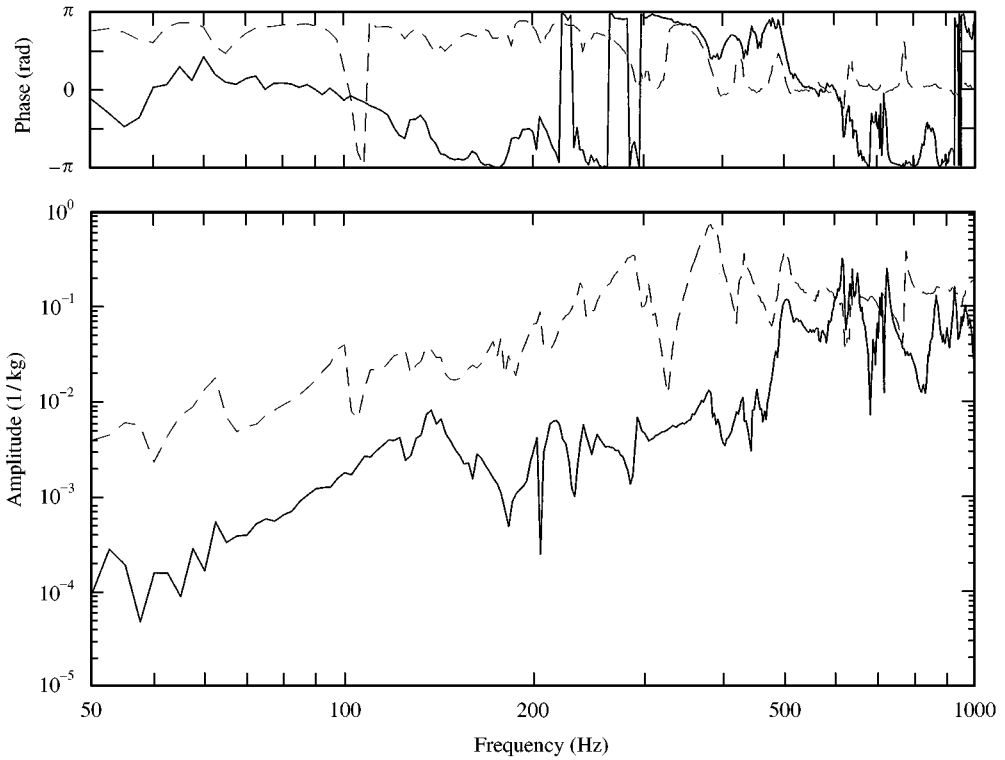


Figure 13. Examples of acceleration  $A_{ij}$  of the pipe system: ----,  $a_7/F_1$ ; ---,  $a_1/F_4$ .

#### 4.3. RESULTS USING SUBSETS OF RESPONSE POSITIONS

When using the response positions in set 1 (positions at D and E) the  $[A]$  matrix has dimensions  $8 \times 6$ . Predictions and measurements are compared in Figure 14. The predicted levels are generally too low, with a deviation of more than 10 dB at 50 Hz. The 95% confidence intervals shown are dominated by the covariance matrix of the response fit. The rank in this case, as given by the number of singular values used in the pseudo-inverse, is 5 or 6 over most of the frequency range. This indicates that the forces cover roughly independent degrees of freedom.

Figure 15 shows results using the response positions of set 2, which are further from the equivalent force locations. These results appear somewhat better than using set 1, particularly for hydrophone position 1. The rank in this case was reduced to 3 or 4 at most frequencies.

#### 4.4. RESULTS USING ALL FORCE AND RESPONSE POSITIONS

A prediction was then carried out when using all 14 response positions. This gave results, not shown, which were little different from those when using set 1. Inspection of the operational responses, however, showed that those at D were 10–20 dB higher than those at other positions. Therefore, the least-squares fit tends

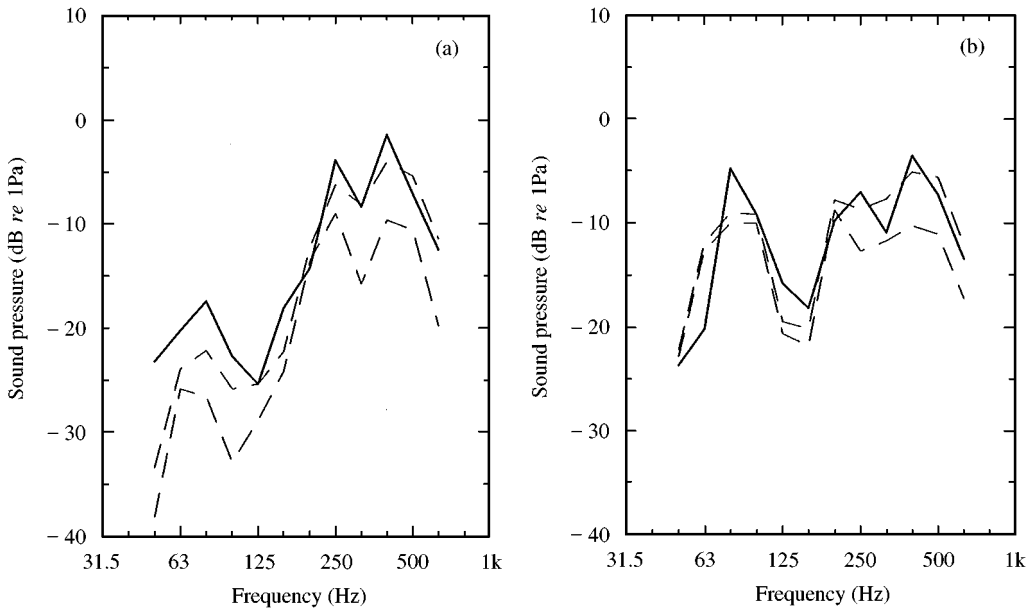


Figure 14. Measured and calculated underwater sound for the pipe system using response points in set 1: —, measured; ---, calculated, 95% confidence interval. (a) underwater position 1. (b) underwater position 2.

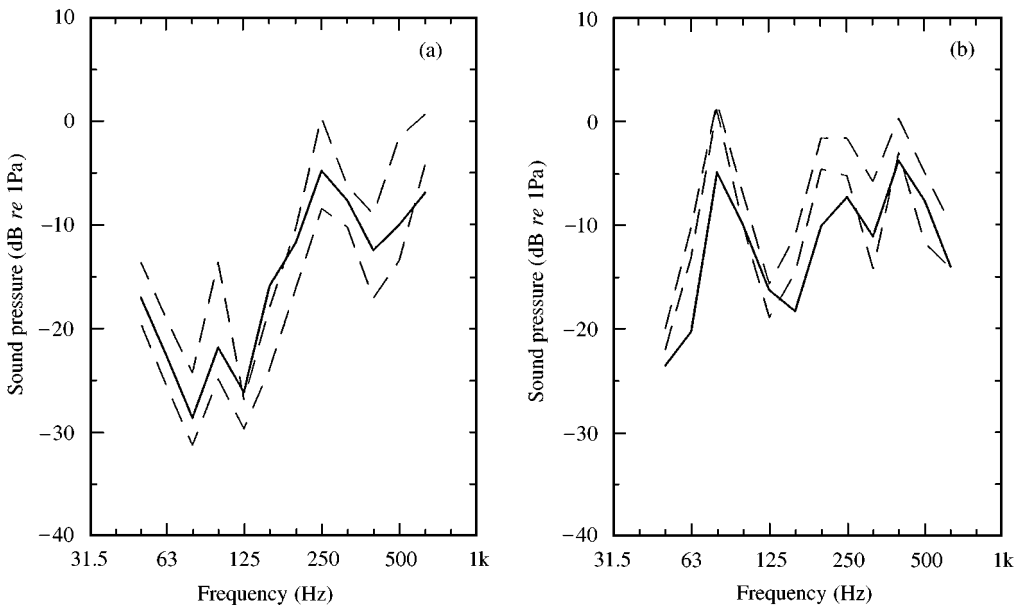


Figure 15. Measured and calculated underwater sound for the pipe system using response points in set 2: —, measured; ---, calculated, 95% confidence interval. (a) underwater position 1. (b) underwater position 2.

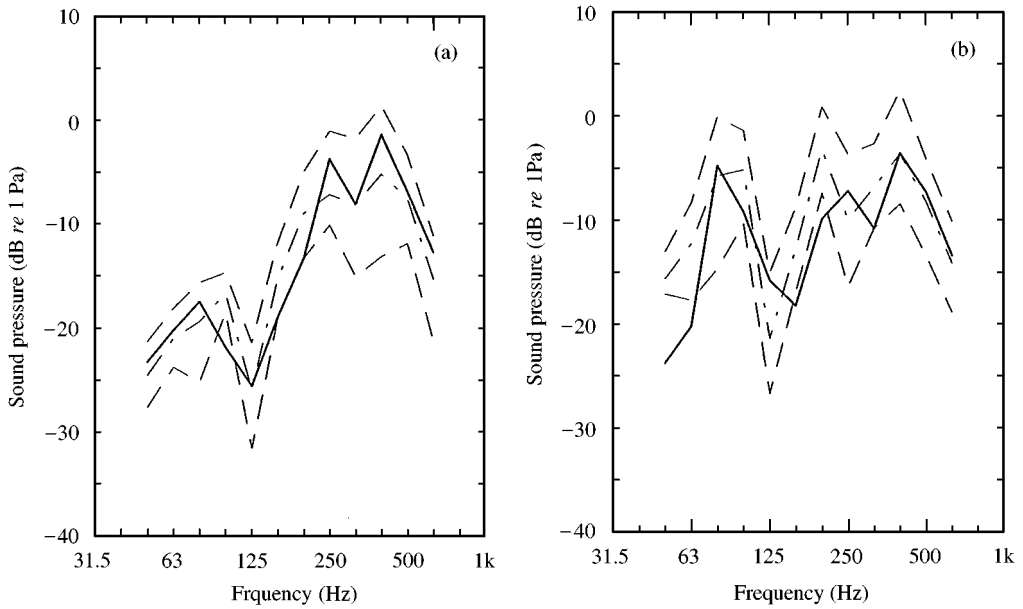


Figure 16. Measured and calculated underwater sound for the pipe system using all 14 responses with weighting applied: —, measured; ---, calculated; mean; ---, calculated, 68% confidence interval. (a) underwater position 1. (b) underwater position 2.

to be dominated by these positions leaving the *relative* error at other positions greater (the absolute error being the same order of magnitude).

To overcome this, the responses were weighted by dividing each row of  $[A_{ij}]$  by its norm. The same weighting factors were applied to the elements of  $\{a_i\}_{mach}$ . Figure 16 shows the results of using this weighting with all 14 response positions included in the analysis. Compared to Figure 15, the mean predictions have been improved significantly. However, the variance of the predictions is increased markedly by this process.

The fact that the confidence interval is much wider in the weighted analysis than in the results for the drive shaft, and that on the other hand the rank is mostly full ( $r = 6$ ), suggests that the six available substitution sources were insufficient to reproduce the vibration field sufficiently well.

#### 4.5. SIMULATIONS

It has been seen that six substitution forces appear to be insufficient to reproduce the vibration of the pipe induced by the “machine”. This indicates that more than six degrees-of-freedom play a role in the sound transmission through the pipe. The cut-on frequency for the  $n = 2$  lobar waves in the pipe is estimated as 1165 Hz, which is outside the frequency range studied. It can be expected, therefore, that the pipe can be modelled as a beam in this frequency region, exhibiting six degrees of freedom. However, coupling with the fluid provides a seventh degree of freedom. To study this possibility further, a numerical simulation was performed.

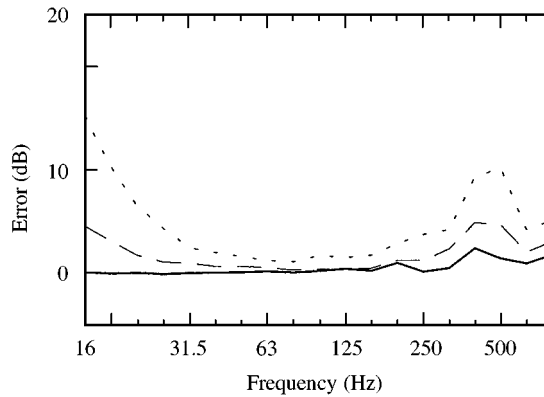


Figure 17. Results for pipe system simulation: average absolute deviation between actual and reconstructed responses; —, deviation at structural positions included in force determination; ---, deviation at structural positions not included in force determination; ···, deviation at fluid-borne positions within the pipe.

Use has been made of a simulation model based on the transfer matrix method and known as PRESTO [22, 23]. This has been used to represent a water-filled pipe system with properties and dimensions equivalent to the system shown in Figure 12, although only the section downstream of the bellows. The source end of the pipe is terminated with a massless end plate connected to the rest of the pipe by a short rubber hose. The system is excited by simultaneous imposed unit translation of this end plate in three orthogonal directions. This represents the “machine” excitation. The responses of the pipe wall in six directions and the response of the fluid within the pipe to the end plate excitation were calculated at seven cross-sections along the pipe.

Simulations were then performed in which equivalent force positions,  $j$ , are chosen along with a corresponding set of response positions,  $i$ . Matrices  $A_{ij}$  of accelerances are obtained from the model, and used in combination with the responses to the “machine” excitation in an equivalent force procedure in an attempt to reconstruct the vibration and sound field in the pipe.

In the first such simulation, six equivalent force positions were located at a cross-section near the beginning of the pipe. Then by using the equivalent forces method with simulated accelerances, a set of forces was derived by using a subset of the available response positions. The results were assessed by studying the quality of the reproduction of the response field. Figure 17 presents the average absolute deviation between the actual responses and the reconstructed responses. Three lines are given. The solid line represents the average fit on the 24 structure-borne response positions used in determining the equivalent forces. These are fitted quite well. The dashed line gives the average results for the structure-borne responses at a further set of 18 positions which are *not* included in the derivation of the equivalent forces. Deviations of up to 5 dB occurred for this situation. Finally, the dotted line presents the error in the reconstruction of the seven fluid-borne responses in the pipe, which shows deviations of up to 10 dB.

In a second simulation, the same procedure was used for a pipe filled with air. In this case all 42 structure-borne responses were reconstructed exactly by the six forces. This shows that it is the additional degree of freedom in the fluid which introduces the errors seen in Figure 17.

In a third simulation, now again for a water-filled pipe, an additional equivalent force position on the pipe surface was added, at a different cross-section from the other six. This allowed an additional degree of freedom to be covered. In this case, all responses, including fluid-borne responses, at cross-sections “down stream” of the force positions were fitted perfectly by the equivalent force procedure.

Of course, these simulation are based on “perfect” data—the addition of random noise would clearly introduce errors into this reconstruction. This could be a useful extension of the study.

To summarize, it can be stated that it is necessary to cover seven degrees of freedom for fluid-filled pipe systems, such as studied here. It is, however, not absolutely necessary to include fluid-borne excitation or response positions, as shown by the third simulation.

## 5. CONCLUDING REMARKS

An equivalent forces method for quantifying structural sound transmission paths has been described. It has been applied successfully to laboratory situations representative of applications in ships. Although beyond the scope of this paper, the method has subsequently been used successfully on board ship for studying the contributions of the drive shaft, cooling water pipes and engine mounting points [9]. The method is well suited to ship-board applications where it is often not possible to dismantle paths or where the impedance mismatch between flexible isolators and receiver structures is small, preventing the use of traditional methods. The use of reciprocity allows the number of accessible force positions to be increased considerably. The method adopted is shown to be a practical approach, which is much less demanding than impedance methods which have to take account of many components of the driving point and transfer impedance matrices [1].

The two examples studied were chosen because of their relevance to the noise transmitted by an engine on board a ship. Of these two examples, the first has been seen to reduce to a fairly simple case with an obvious single connection point between source and receiver. Moments and in-plane forces were shown in this case to be much less significant than the two transverse force directions. However, the second example is much more complex, with multiple-degree-of-freedom structural vibrations occurring together with fluid-borne transmission. This was further complicated by the introduction of an overpressure in the fluid which modified the transmission path between the two parts of the experiment. It is therefore perhaps not so surprising that the results are more disappointing in this case. It would be of interest in further work to study an intermediate case, for example a two-dimensional system such as a rod with a bend between the source and receiver structure.

It has been shown that the use of a multi-degree-of-freedom approach to mechanical substitution sources is essential in the applications considered. For the drive shaft bearing two excitation degrees of freedom sufficed but for the pipe even six was insufficient, as also demonstrated by simulations. Finding an appropriate source model, in particular the choice of force and response positions, remains partly intuitive, although in practice the freedom to choose these will be limited by accessibility.

A methodology has been developed for determining the confidence intervals of the results. This requires the simultaneous measurement of operational responses at all positions in order to determine the covariance matrix. Also the variance of fit is used, which gives an indication of the suitability of the choice of the source modelling, i.e. force and response positions chosen. Inspection of the rank also gives an indication of whether the system is sufficiently well defined by the co-ordinates chosen. These measures assist in the assessment and possible improvement of the source modelling.

#### ACKNOWLEDGMENTS

The work described here formed part of a programme named Advanced Noise Transmission Experimentation and Analysis for Signature Reduction (ANTEASR), supervised by representatives of the US Navy and the Royal Netherlands Navy. Technical guidance was given by staff members of the former David Taylor Research Center, now Naval Surface Warfare Center, Carderock Division. The authors are grateful to the many colleagues who contributed to the experiments. The helpful suggestions of the referees are kindly acknowledged.

#### REFERENCES

1. J. W. VERHEIJ 1982 *Doctoral thesis, TNO Institute of Applied Physics*. Multipath sound transfer from resiliently mounted shipboard machinery.
2. J. W. VERHEIJ 1997 *International Journal of Acoustics and Vibration* **2**, 11–20. Inverse and reciprocity methods for noise source characterization and path quantification. Part 1: Sources.
3. J. M. MONDOT and B. A. T. PETERSSON 1987 *Journal of Sound and Vibration* **114**, 507–518. Characterization of structure-borne sound sources: the source descriptor and the coupling function.
4. U. FINGBERG and T. AHLERSMEYER 1992 *Proceedings of the 17th International Seminar on Modal Analysis, Leuven, Belgium*, 143–152. Noise path analysis of structure-borne engine excitation to interior noise of a vehicle.
5. H. VAN DER AUWERAER, K. WYCKAERT, W. HENDRICKX and P. VAN DER LINDEN 1995 *Proceedings International Seminar on Applied Acoustics ISAAC 6, Leuven*, vol IV, 1–22. Noise and vibration transfer path analysis.
6. P. MAS, P. SAS and K. WYCKAERT 1994 *Proceedings of the 19th International Seminar on Modal Analysis, Leuven, Belgium*, 1049–1065. Indirect force identification based on impedance matrix inversion: a study on statistical and deterministic accuracy.
7. J. ROMANO and J. A. LÓPEZ 1996 *Proceedings of the 21st International Seminar on Modal Analysis, Leuven, Belgium*, 527–536. Practical application of transfer path analysis to resolve structure-borne noise problems in vehicle design.

8. G. KONERS 1996 *Proceedings of the 21st International Seminar on Modal Analysis, Leuven, Belgium*, 1377–1387. Improvement of the 2nd EO booming noise of a diesel engine car. Application of TPA including structure-borne and airborne noise.
9. J. W. VERHEIJ 1997 *International Journal of Acoustics and Vibration* **2**, 103–112. Inverse and reciprocity methods for noise source characterization and path quantification. Part 2: Transmission paths.
10. U. FINGBERG 1994 *Proceedings of the 19th International Seminar on Modal Analysis, Leuven, Belgium*, 899–910. Road/tyre noise development using noise path analysis techniques.
11. M. H. A. JANSSENS and J. W. VERHEIJ 1997 *Proceedings of Internoise 97, Budapest, Hungary*, 1335–1338. The pseudo-forces method for characterizing the source-strength for structure-borne sound.
12. F. J. FAHY 1995 *Acustica* **81**, 544–558. The vibro-acoustic reciprocity principle and applications to noise control.
13. I. L. VÉR 1992 in *Noise and Vibration Control Engineering, Principles and Applications*, L. L. BERANEK and I. L. VÉR (editors) New York: Wiley, Chapter 9. Interaction of sound waves with solid structures.
14. B. J. DOBSON and E. RIDER 1990 *Proceedings of the Institution of Mechanical Engineers part C Journal of Mechanical Engineering Science* **204**, 69–75. A review of the indirect calculation of excitation forces from measured structural response data.
15. J. M. STARKEY and G. L. MERRILL 1989 *International Journal of Modal Analysis* **4**, 103–108. On the ill-conditioned nature of indirect force measurement techniques.
16. T. J. ROGGENKAMP and R. J. BERNHARD 1993 *Proceedings of Internoise 93, Leuven, Belgium*, 881–884. Indirect measurement of multiple random force spectra.
17. W. H. PRESS *et al* 1986 *Numerical Recipes: The Art of Scientific Computing*. Cambridge: Cambridge University Press.
18. R. E. POWELL 1982 *Doctoral thesis, Massachusetts Institute of Technology*. Multichannel inverse filtering of machinery vibration signals.
19. R. E. POWELL and W. SEERING 1984 *Transactions of the ASME, Journal of Vibration, Acoustics, Stress and Reliability in Design* **106**, 22–28. Multichannel structural inverse filtering.
20. N. R. DRAPER and H. SMITH 1981 *Applied Regression Analysis*. New York: Wiley, second edition.
21. M. R. SPIEGEL 1972 *Theory and Problems of Statistics* (Schaum's Outline Series) New York: McGraw-Hill.
22. C. A. F. DE JONG 1994 *Doctoral Thesis, TNO Institute of Applied Physics, Delft*, Analysis of pulsations and vibrations in fluid-filled pipe systems.
23. C. A. F. DE JONG and M. H. A. JANSSENS 1996 *Proceedings of Internoise 96, Liverpool, UK*, 3203–3206. Numerical studies of inverse methods for quantification of sound transmission along fluid-filled pipes.